

Confirmation of a moving component in the H α emission line of LS I+61⁰303

Radoslav K. Zamanov

National Astronomical Observatory Rozhen, 4700 Smoljan, Bulgaria

Josep Martí

Dep. Física, Univ. de Jaén, Virgen de la Cabeza 2, 23071 Jaén, Spain

Abstract. We report our attempts to detect and confirm a narrow moving component in the H α emission line of LS I+61⁰303. The existence of this spectral feature was already suspected in the past. As a result, we find that this component does exist and that its radial velocity varies in agreement with the radio period of the system. We interpret it tentatively as due to a denser region, or bulge, orbiting near the outer edge of the H α emitting disk.

1. Introduction

LS I+61⁰303 (V615 Cas, GT 0236+610) is a radio emitting Be/X-ray binary, with its primary being a rapidly rotating B0V star with an equatorial disk. The secondary is a compact object, most probably a neutron star, orbiting in an eccentric orbit. The most spectacular phenomena associated with this object are its periodic non-thermal radio outbursts, repeating every ~ 26.5 d. This interval is supposed to be the orbital period of the binary.

The H α of LS I+61⁰303 is observed as a double peaked emission line of variable profile intensity which is not peculiar with respect to those observed in other Be stars. High resolution H α observations of this object are discussed in few papers (Paredes et al. 1994, Zamanov et al. 1999). In these papers, variability of the H α emission line was established over time scales of days and two possible interpretations were proposed to account for it, namely: (i) an influence of the compact object onto the Be star disk; (ii) an unresolved emission line component due to gas within the system or ejected from it.

The present paper discusses H α observations of LS I+61⁰303 with the aim of testing the reality of proposed unresolved component.

2. Observations, data reduction and results

The observations were obtained with the Coudé spectrograph of the 2 m telescope at the Bulgarian NAO “Rozhen”. They cover about 110 Å (0.2 Å pixel⁻¹) and have a signal-to-noise ratio in the range 30-50. In order to detect a possible narrow or unresolved component we have applied the following procedure:

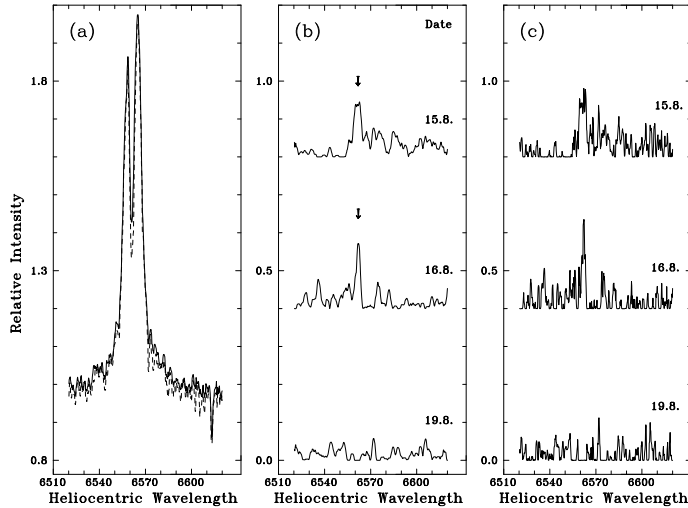


Figure 1. **(a)** An example of average spectrum (solid line) and the “minimum spectrum” (dashed line) obtained using the spectra from 15, 16 and 19 August 1997. **(b)** The smoothed residuals for the same group. The arrows indicate the positions of the moving component. **(c)** The unsmoothed residuals for the same spectra. The plots are offset by adding arbitrary constants identical for panels (b) and (c).

1. All spectra were transformed to an uniform heliocentric wavelength set.
2. The spectra were divided into 10 groups. Every group consists of 3-4 spectra, obtained in consecutive or close nights. For each group the “minimum spectrum” was generated by taking the minimum pixel intensity from all the spectra of the group over the uniform wavelength set.
3. The “minimum spectrum” was subtracted from all spectra in the group. The residuals were smoothed with a moving average over 10-15 points (2 to 3 Å). An example is shown in Fig. 1.

The applied procedure assumes explicitly that, if moving component exists, it must appear as a pure emission line (not absorption).

It is visible in Fig. 1 that a moving narrow component does exist. This feature clearly shows up in most residual plots after the “minimum spectrum” is subtracted. The typical FWHM of this moving component is 4-8 Å, with a normalized intensity about 0.1-0.2. The radial velocity of the component was determined by employing a Gaussian fit, with a typical error of $\pm 50 \text{ km s}^{-1}$. We plotted our measurements in the left panel of Fig. 2 folded on the radio phase of LS I+61°303. The latest ephemeris by Gregory et al. (1999) was used for this purpose, with the phase origin set at JD 2443366.775 and a 26.4917 d radio period being adopted. A clear trend of the component radial velocity emerges in this figure. Indeed, a modulation with the same 26.5 d radio period and a $\pm 250 \text{ km s}^{-1}$ amplitude seems to be present in the data. Such a strong radial velocity dependence gives us confidence that we are detecting a real variability, and that this is not likely to be an artifact of the applied procedure. It deserves to be noted here that the moving component was already directly visible in the

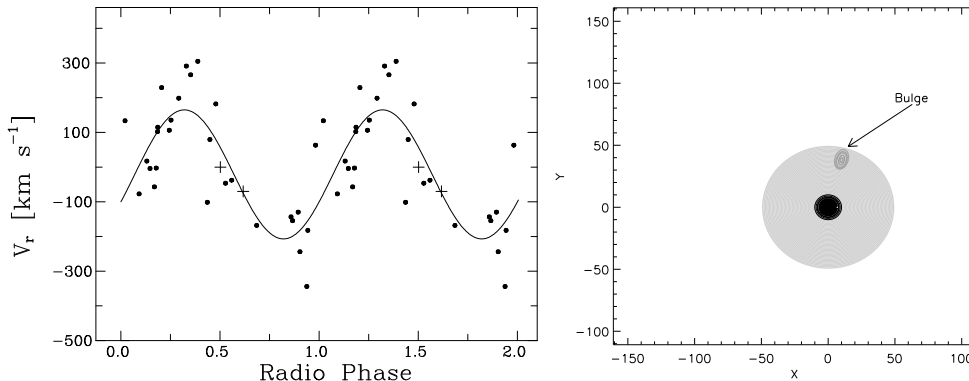


Figure 2. **Left panel:** Phase plot of the radial velocities of the moving component as a function of radio phase. The solid line is the best cosine fit. The dots represent our data, the crosses - from Paredes et al. (1990). **Right panel:** Schematic representation of the Be star, its $H\alpha$ -emitting disk, and the bulge located near to the outer edge. The axes are in units of R_{\odot} .

high resolution spectra of Paredes et al. (1990), and without any subtraction procedure being applied. The radial velocity measurements of these authors have been incorporated in Fig. 2 and they are in excellent agreement with our observations.

By fitting to the data points a least squares cosine function of the form: $V_r(\varphi) = A + B \cos [2\pi(\varphi - \varphi_0)]$, we obtain the following best fit parameters: $A = -21 \pm 14 \text{ km s}^{-1}$, $B = 186 \pm 20 \text{ km s}^{-1}$, and a phase shift $\varphi_0 = 0.68 \pm 0.02$ (φ is the radio phase). As it can be expected, the parameter A is near to the system velocity -55 km s^{-1} derived by Hutchings & Crampton (1981). The best fit cosine fit is plotted in Fig. 2 as a solid line.

3. Discussion

What is the origin of the moving component? Among possible interpretations, one could think of a possible relationship with the compact companion in the LS I+61°303 system, i.e., due to matter captured by the neutron star from the Be star wind - the material around the neutron star, or an accretion disk, or an accretion wake.

The orbital parameters of LS I+61°303 are not well constrained so far. The proposed orbits by Hutchings & Crampton (1981) and Martí & Paredes (1995) are quite different. In spite of this uncertainty, the observed variations up to $\pm 250 \text{ km s}^{-1}$ are significantly larger than those expected from the orbital motion of the neutron star, as well as of the Be star, in all proposed orbital solutions. Consequently a direct relationship, in the sense that the moving component is reflecting the motion of the neutron star, does not seem to apply unless the orbit is extremely eccentric, and alternative interpretations need to be considered.

The spectrally resolved interferometry of ζ Tauri by Vakili et al. (1998) has shown a bulge of emission in the disk of this Be star. These authors have

interpreted their interferometric and $H\alpha$ observations assuming that such a bulge follows a circular orbit in the equatorial disk plane, at a distance of about 7 stellar radii from the central star. In this context, it is thus conceivable to us that the moving $H\alpha$ component in LS I+61°303 is also due to a bulge region existing in the circumstellar disk.

Under the assumption that this is the case, let us find the position of the bulge. Hereafter, we will adopt the following parameters for the Be star in LS I+61°303: $M_* = 10 M_\odot$, $R_* = 10 R_\odot$, and $v \sin i = 360 \text{ km s}^{-1}$ (Hutchings & Crampton 1981). Assuming that the star rotates at 90% of its critical velocity (Sletteback et al. 1992), we derive $\sin i = 0.92$ and $i \simeq 67^\circ$. Consequently, from the term B in Eq. 1 and the above assumptions we obtain that the bulge in LS I+61°303 rotates at a velocity $V_{\text{bulge}} = B/\sin i = 202 \text{ km s}^{-1}$. This corresponds to a distance of about $\sim 4.5 R_*$, provided that the bulge is in a Keplerian orbit around the star.

From the relationship between the separation of the $H\alpha$ peaks, ΔV_{peak} , and the outer radius R_{out} of a Keplerian emitting disk: $R_{\text{out}} = R_*(2v \sin i / \Delta V_{\text{peak}})^2$, we find that $R_{\text{out}} = 4.0\text{-}6.6 R_*$ (using $\Delta V_{\text{peak}} = 300\text{-}360 \text{ km s}^{-1}$, Zamanov et al. 1999). This result compares satisfactorily to the bulge distance found above and implies that the bulge must be located near to the outer edge of the $H\alpha$ emitting disk. A schematic picture of the $H\alpha$ disk and the position of the bulge is represented in the right panel of Fig. 2.

As mentioned before, the orbital elements of the Be X-ray binary LS I+61°303 are not well determined. From the 26.5 d period present in the V_r data, one could wonder if the position of the bulge should be in phase with the motion of the neutron star. However, this does not occur in any of the proposed orbital solutions. Whether at the end there is a relationship between the bulge position and that of the neutron star remains to be determined by a careful revision of orbital solutions in the future.

Acknowledgements: RZ acknowledges support by IAU Grant and by Bulgarian NSF (MUF-05/96). JM is supported by DGICYT (PB97-0903) and by Junta de Andalucía (Spain).

References

- Gregory P.C., Peracaula M., Taylor A.R. 1999, ApJ, in press
 Hutchings J.B., Crampton D. 1981, PASP, 93, 486
 Martí J., Paredes J.M. 1995, A&A, 298, 151
 Paredes J.M., Marziani P., Figueras F., Jordi C., Martí J., Rosselló G. et al. 1990, Boletín Astronómico del Observatorio de Madrid, v.XII, N:3, 191
 Paredes J.M., Marziani P., Martí J., Fabregat J., et al. 1994, A&A, 288, 519
 Sletteback A., Collins II G.W., Truax R., 1992, ApJS, 81, 335
 Vakili F., Mourard D., Stee Ph., Bonneau D., et al. 1998, A&A, 335, 261
 Zamanov R., Martí J., Paredes J.M., Fabregat J., Ribó J., Tarasov, A.E., 1999, A&A, in press

Table 1. Radial velocities of the moving component

JD2400000+	V_r [km/s]	Group	JD2400000+	V_r [km/s]	Group
49292.31	266	1	50293.55	-77	7
49293.27	305	1	50294.57	17	7
49294.53	-101	1	50298.58	-	7
49354.21	-168	2	50320.58	-	8
49356.26	-	2	50321.53	-3	8
49374.48	79	3	50322.37	-2	8
49375.25	182	3	50322.53	102	8
49385.33	-143	3	50322.56	114	8
49386.26	-129	3	50676.52	31	9
49528.45	135	4	50677.36	-26	9
49529.47	198	4	50680.56	187	9
49530.48	291	4	50685.49	-222	9
49531.42	-	4	50686.47	-260	9
50181.29	-	5	50687.55	-197	9
50182.26	-	5	50688.59	-76	9
50183.35	-344	5	50689.60	77	9
50242.53	-57	6	50703.38	-293	10
50243.52	229	6	50704.56	326	10
50244.52	106	6	50705.54	216	10